



23 the seepage of aquifer water was decomposed into lateral and vertical transport, and
24 the two kinds of "lagging" transport processes were superimposed to obtain the final
25 groundwater level tidal response, which may appear as an anomalous phenomenon in
26 which the phase is over the front after superposition. Taking the Lugu Lake well as an
27 example, before the Wenchuan earthquake, the phase of groundwater level was ahead
28 of the theoretical solid tide, indicating the existence of a transgressive aquifer,
29 whereas the groundwater level tidal factor declined from 0.28 mm/uGal before the
30 earthquake to 0.23 mm/uGal after the earthquake. The phase, from 15 min ahead in
31 pre-earthquake to 15 min lagged after the earthquake, combined with the theoretical
32 analysis it can be seen that the Wenchuan earthquake led to develop the new fissure in
33 the Lugu Lake well, thus permanently altering its aquifer response and changing the
34 permeability of the aquifer. However, the subsequent earthquakes did not produce
35 new fissures; only the seismic waves caused by the stress redistribution process were
36 observed. This co-seismic response of the groundwater level shows a step-down
37 phenomenon, phase analysis of the groundwater level has scientific significance for
38 the study of well-aquifer conditions and well-borehole seismic capacity.

39

40 **【Key Words】** Groundwater level tidal; Tide factor; The phase; co-seismic response

41

42 **1. Introduction**

43 The quantitative analysis of groundwater levels in unconfined boreholes as
44 affected by Earth solid tides and atmospheric pressure is a classical problem in the
45 hydrogeological and seismic subsurface fluid disciplines. Efforts have been made for



46 the theoretical calculations and characterization (Gulley et al., 2013; Liu et al., 2017;
47 Lee et al., 2017; He et al., 2020; Yan et al., 2020; Ma et al., 2023). Earth solid tides
48 are characterized by fixed periods and amplitudes, and the tidal response of
49 groundwater level can be conveniently utilized for quantitative calculation of
50 well-aquifer structural parameters. Cooper et al. (1965) derived an equation of motion
51 for the water column in the well and a method for the calculation of the aquifer
52 transmissivity (T) and aquifer storage rate (S). The groundwater level has zero delay
53 property for ground vibration in a certain frequency range (He et al., 2017), and the
54 groundwater level tidal response has the same frequency as the Earth's solid tides. It is
55 expressed as a sum of harmonics, which only differs in amplitude and phase (Cooper
56 et al., 1965). Hsieh et al. (1987) gave a formula for calculating the amplitude and
57 phase of the tidal response of the water level in wells. The amplitude of the vibration
58 of the water level in wells is mainly affected by the characteristic parameters of elastic
59 deformation of the aquifer, such as Skempton's coefficient, bulk modulus, and
60 Poisson's ratio (Ding et al., 2015; Arditty et al., 1978; Bredehoeft, 1967; Burbey, 2010;
61 Sato et al., 2006; Gao et al., 2020; Van der Kamp and Gale, 1983; All ègre et al., 2016);
62 and the phase is mainly related to the water flow properties of the aquifer, such as
63 permeability (Zhu et al., 2021; Elkhoury et al., 2006; Lai et al., 2014; Shi et al., 2014;
64 Xue et al., 2013; Zhu, 2021).

65 Assuming that the aquifer is confined, laterally extended, homogeneous, and
66 isotropic, Hsieh et al. (1987) utilized the diffusion equation to derive the phase lag of
67 the tidal response of the water level in the well as a function of aquifer permeability,
68 storage rate, and Earth's solids tides, and there is always a phase lag in water level
69 tidal response of wells because it takes a certain amount of time for the fluids in the

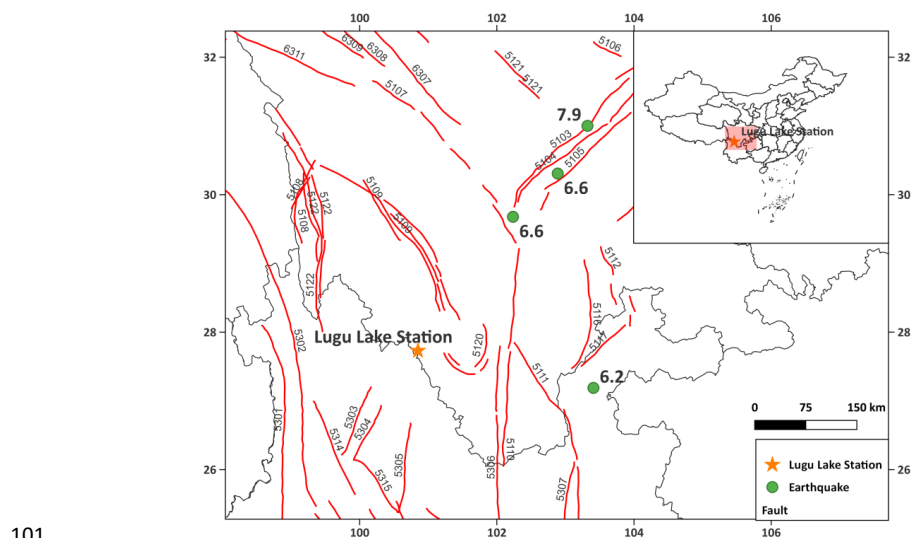


70 aquifer to respond to the tidal force and flow into or out of the wells. Chinese scholars
71 have also obtained a similar understanding through theoretical analysis, that is, the
72 inelastic response of the aquifer system to the tidal force leads to a phase difference in
73 the tidal response of the water level in the wells, the size of which mainly depends on
74 the radius of the borehole and the permeability of the aquifer (Zhang et al., 1991;
75 Zhou et al., 1993), but there is no reasonable explanation for the phase overshooting
76 of the tidal response of the wells' water levels. Maas and De Lange (1987) derived the
77 phase shift and attenuation equations in the case of a weakly permeable layer
78 overlying a single aquifer using the superposition principle. Studies comprehensively
79 show that phase lead in the tidal response of groundwater level is due to the
80 semi-confined aquifer with weakly permeable water quality. Studies on the conditions
81 for the existence of phase lead have been carried out using numerical simulations
82 from the theoretical aspect by above authors; however, reports on how to reflect this
83 in the analysis of the actual data and carry out response decomposition of the different
84 layers of the aquifer from the actual observation data of the water level of wells are
85 lacking. In the present study, our efforts are to explain the phase lead of the tidal
86 response of the groundwater level by combining the actual situation of the borehole
87 and groundwater level observation from China Earthquake Networks Center.

88 The water level data from the Lugu Lake seismic station (51306, Figure 1)
89 (N27.73 °, E100.85 °) is considered as an example for analysis. This station exposed
90 strata is sandstone of the upper diamictic Black Mud Whistle Formation (P2h) and the
91 sand and gravel layers of alluvial, flood, lacustrine, and slope deposits. Tectonically, it
92 is located in the two flanks of the Yanyuan Arc Tectonic Belt, and the nearby fractures
93 mainly include the Dog Drilling Cave - Cat's Home Village, Gaizu-Xizhu, and
94 Bleaching fractures. The fracture in this region is a positive fracture. The depth of the



95 borehole is 200.7 m, with 61 m of clay cover, under which is tuff. The depth of the
96 casing is 74.2 m, and process of stopping water is adopted by the piston pressure of
97 the casing reserved hole in the bottom section of the borehole until the cement slurry
98 is returned from the ground to reduce the interference of the surface water on the
99 water level of the borehole. The pumping experiment at the borehole completion
100 showed that the permeability coefficient was 0.135 m/d.



101

102 **Figure 1. Distribution of earthquakes in and around the Lugu Lake Seismic Station**

103 (5103, 5104, 5105: Longmenshan fault zone; 5110: Annin River fault zone; 5109: Litang-Derwu fault zone; 5122:

104 Jinsha River fault zone)

105 The water level observation of the Lugu Lake station started in December 2007.
106 The water level data have 1-min sampling intervals with a resolution of 1 mm. The
107 precise time was determined using a Global Positioning System (GPS) or Simple
108 Network Time Protocol (SNTP) to ensure temporal consistency with a resolution
109 and accuracy of 5 s. The seismic events with magnitudes greater than 6.2 (Table 1)
110 were selected for analysis within 500 km around the Lugu Lake station.

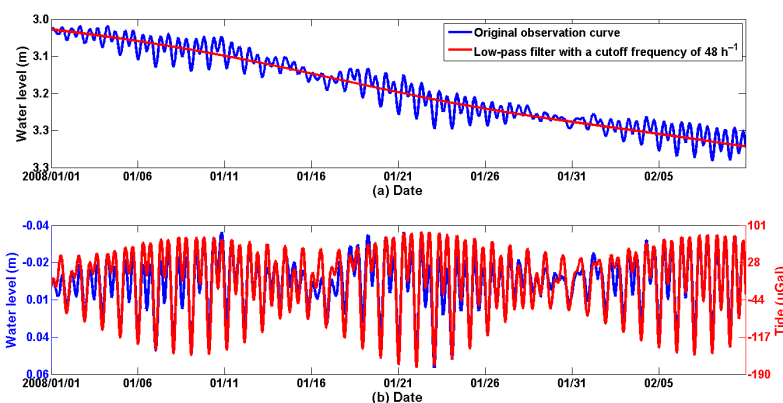


111 Table 1. Seismic events with magnitudes greater than 6.2 within 500 km around the Lugu Lake
112 Station

| Identifier | Time | Latitude | Longitude | Mag (mw) | Distance (km) | Location |
|------------|------------------|----------|-----------|----------|---------------|------------------------------|
| EQ1 | 2008-05-12 14:28 | 31.002 | 103.322 | 7.9 | 437 | 58 km W of Tianpeng, China |
| EQ2 | 2013-04-20 08:02 | 30.308 | 102.888 | 6.6 | 350 | 56 km WSW of Linqiong, China |
| EQ3 | 2014-08-03 16:30 | 27.1891 | 103.4086 | 6.2 | 258 | 33 km WSW of Zhaotong, China |
| EQ4 | 2022-09-05 12:52 | 29.6786 | 102.236 | 6.6 | 257 | 44 km SE of Kangding, China |

113 2. Method

114 In order to calculate the tidal response parameters of the well water level more
115 accurately, a low-pass filter with a cut-off frequency of 48h^{-1} is used to extract the
116 trend of the well water level. Then, the low-frequency data is subtracted from the
117 original data, and only the tidal components of the well water level is retained (Figure
118 2).



119

120 Figure 2. Tidal components of the well water level is retained

121 The `t_tide` tool provided by Pawlowicz et al. (2002) was used to calculate the
122 magnitude and phase of each tidal sub-wave (Figure 3), which was carried out by
123 comparing the groundwater level and theoretical solid gravity tide to make the

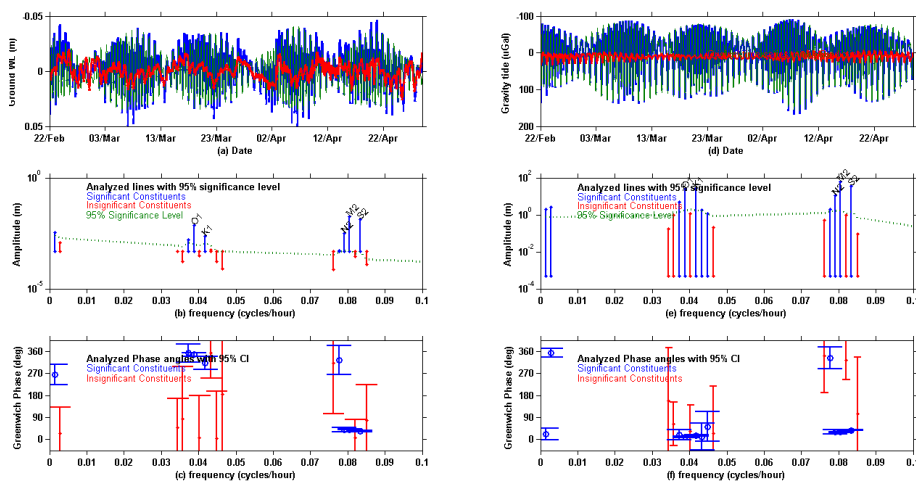


124 magnitude and phase comparable in the time series. For example, for the M2 wave
 125 (period of 12.42 h), the magnitude and phase parameters of the groundwater level and
 126 the solid gravity tide were calculated separately using the `t_tide` tool and then
 127 according to Equation (1).

$$f = A_w/A_g \tag{1}$$

$$\varphi_d = \varphi_w - \varphi_g$$

128 where f is the groundwater level tidal factor of the M2 wave, A_w and A_g are
 129 the groundwater level and gravity tidal oscillation amplitude in mm and uGal,
 130 respectively. φ_w and φ_g are the phases of groundwater level and M2 sub-wave of
 131 the gravity tidal wave, respectively; φ_d , the phase difference between the
 132 groundwater level and gravity tidal wave is greater than 0 to indicate a phase lead and
 133 less than 0 to indicate a phase lag.



134

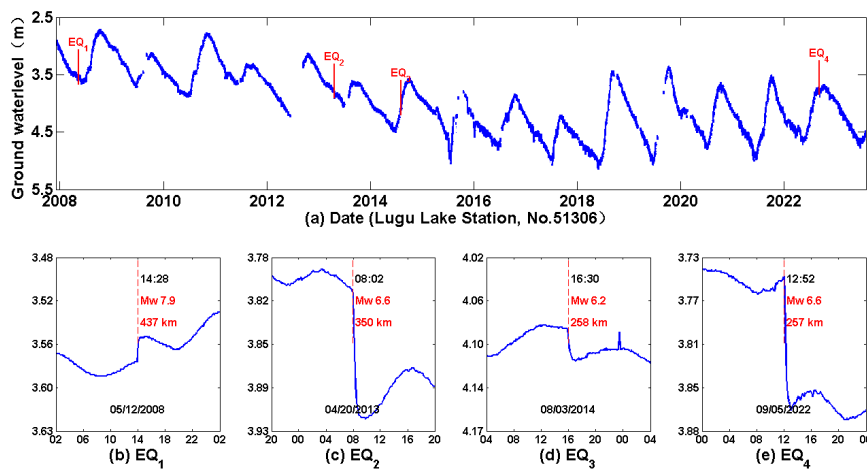
135 **Figure 3. Tidal parameter calculations using the `t_tide` tool for the Lugu Lake Station**
 136 **groundwater level and theoretical gravity tides**



137 **3. Results**

138 The multi-year variability of water level is shown in Figure 4; the annual
139 variation of the water level in the Lugu Lake well is approximately 1 m and a clear
140 solid tide was recorded, that showed an annual variation pattern of high in winter and
141 low in summer. The water level shows less disturbed, the data observed were stable
142 and reliable, in addition to seasonal perturbations.

143 All four selected seismic events show significant coseismic responses,
144 remarkably, the Wenchuan earthquake (Mw 7.9, 437 km) on May 12, 2008 caused a
145 minor step increase in the water level of the well, the other three earthquakes caused
146 significant step decline in the water level, and the magnitude of the step decline of the
147 water level and of the earthquake are found to show a positive correlation.



148

149 **Figure 4. Multi-year variations of water level in the Lugu Lake station and co-seismic**
150 **response to earthquakes**

151 The used data was collected over a period of 60 days for each calculation, e.g.,



152 the result for the data collected from February 21–April 20, 2008 is showed in Table

153 2.

154 Table 2. The results for the data collected from February 21–April 20, 2008

| tide | Period (h) | Groundwater level demodulation | | | | Gravitational tidal demodulation | | | |
|------------|---------------|--------------------------------|----------|-------------|------------|----------------------------------|-------------|-------------|------------|
| | | amp | amp_err | pha | pha_err | amp | amp_err | pha | pha_err |
| MM | 661.29 | 3.3 | 3 | 264.7 | 41.2 | 1.91 | 0.80 | 20.8 | 25.8 |
| MSF | 354.37 | 1.2 | 2 | 23.2 | 104.8 | 2.63 | 0.83 | 354.2 | 15.2 |
| ALP1 | 29.07 | 0.5 | 1 | 48.1 | 101.5 | 0.18 | 1.15 | 157.9 | 213.3 |
| 2Q1 | 28.01 | 0.2 | 1 | 84.5 | 200.2 | 0.99 | 1.51 | 62.8 | 105.3 |
| *Q1 | 26.87 | 1.6 | 1 | 352.4 | 35.4 | 4.77 | 1.52 | 19.6 | 17.6 |
| *O1 | 25.82 | 7.2 | 1 | 346.3 | 8.5 | 25.16 | 1.56 | 9.4 | 3.3 |
| NO1 | 24.83 | 0.3 | 1 | 6.4 | 166.6 | 1.20 | 1.71 | 32.5 | 99.5 |
| *K1 | 23.93 | 2.4 | 1 | 311.6 | 28.3 | 27.94 | 1.68 | 14.8 | 3.5 |
| J1 | 23.1 | 0.6 | 1 | 352.7 | 105.7 | 1.73 | 1.50 | 10.5 | 57.9 |
| OO1 | 22.31 | 0.2 | 1 | 4.0 | 182.9 | 1.10 | 1.12 | 52.6 | 64.6 |
| UPS1 | 21.58 | 0.1 | 0 | 185.6 | 205.8 | 0.20 | 0.74 | 24.7 | 193.6 |
| EPS2 | 13.13 | 0.1 | 0 | 312.0 | 208.3 | 0.52 | 1.22 | 341.5 | 160.0 |
| MU2 | 12.87 | 0.5 | 0 | 324.5 | 52.5 | 2.00 | 1.57 | 332.0 | 42.3 |
| *N2 | 12.66 | 3.3 | 1 | 40.2 | 9.1 | 11.16 | 1.85 | 30.5 | 9.0 |
| *M2 | 12.42 | 17.4 | 1 | 39.7 | 1.7 | 59.10 | 1.73 | 30.5 | 1.8 |
| L2 | 12.19 | 0.3 | 0 | 5.9 | 75.4 | 0.92 | 1.07 | 323.9 | 78.9 |
| *S2 | 12 | 13.3 | 1 | 33.6 | 2.0 | 34.89 | 1.62 | 37.8 | 2.5 |
| ETA2 | 11.75 | 0.1 | 0 | 78.9 | 133.8 | 0.09 | 0.74 | 104.4 | 221.8 |
| MO3 | 8.39 | 0.1 | 0 | 19.9 | 168.4 | 0.21 | 0.08 | 71.4 | 20.6 |
| M3 | 8.28 | 0.2 | 0 | 88.3 | 67.5 | 1.00 | 0.09 | 47.8 | 4.8 |
| MK3 | 8.18 | 0.2 | 0 | 112.6 | 69.6 | 0.03 | 0.06 | 186.6 | 116.1 |
| *SK3 | 7.99 | 0.3 | 0 | 236.8 | 35.5 | 0.04 | 0.06 | 246.9 | 94.7 |
| MN4 | 6.27 | 0.1 | 0 | 36.5 | 54.8 | 0.02 | 0.02 | 112.6 | 41.8 |
| M4 | 6.21 | 0.1 | 0 | 46.4 | 100.3 | 0.02 | 0.01 | 72.7 | 37.6 |
| SN4 | 6.16 | 0.1 | 0 | 1.2 | 74.8 | 0.03 | 0.02 | 7.3 | 28.3 |
| MS4 | 6.1 | 0.1 | 0 | 86.7 | 65.9 | 0.02 | 0.02 | 236.1 | 44.8 |
| S4 | 6 | 0 | 0 | 246.9 | 119.7 | 0.03 | 0.01 | 118.4 | 28.9 |
| 2MK5 | 4.93 | 0 | 0 | 74.3 | 157.2 | 0.02 | 0.01 | 176.3 | 16.8 |
| 2SK5 | 4.8 | 0 | 0 | 35.2 | 156.1 | 0.02 | 0.01 | 220.7 | 20.0 |
| 2MN6 | 4.17 | 0 | 0 | 258.9 | 122.3 | 0.02 | 0.01 | 302.0 | 25.9 |
| M6 | 4.14 | 0 | 0 | 206.7 | 161.9 | 0.01 | 0.01 | 174.6 | 31.6 |
| 2MS6 | 4.09 | 0.1 | 0 | 66.3 | 45.5 | 0.02 | 0.01 | 54.5 | 23.6 |
| 2SM6 | 4.05 | 0 | 0 | 275.0 | 89.4 | 0.01 | 0.01 | 232.5 | 39.7 |
| 3MK7 | 3.53 | 0 | 0 | 265.0 | 128.0 | 0.01 | 0.00 | 315.2 | 11.1 |
| M8 | 3.11 | 0.1 | 0 | 36.9 | 48.7 | 0.01 | 0.00 | 357.6 | 3.4 |

155 Calculating the M2 wave tidal parameters for February 21-April 20, 2008,

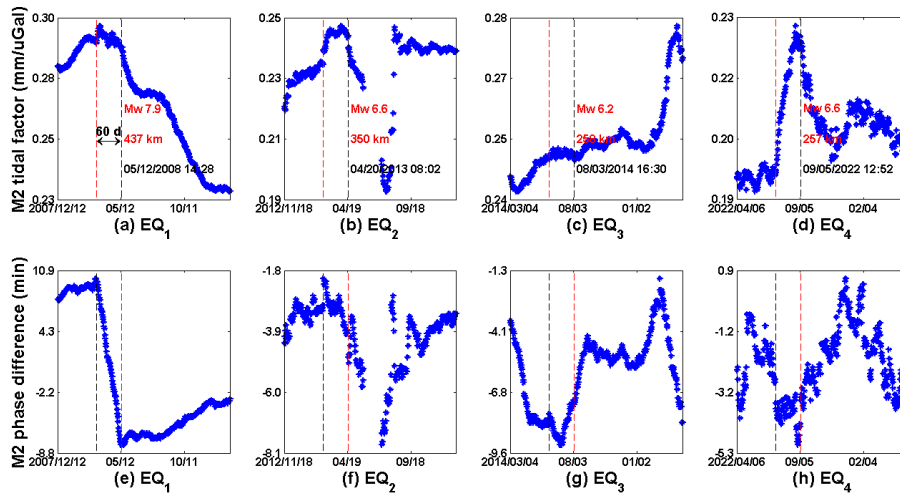
156 according to Equation (1):



$$f = \frac{A_w}{A_g} = \frac{17.4\text{mm}}{59.10\text{uGal}} = 0.2944 \text{ mm/uGal}$$

$$\varphi_d = \varphi_w - \varphi_g = 39.7 - 30.5 = 9.2^\circ = \frac{9.2}{360} * 12.42 * 60 \approx 19 \text{ min}$$

157 Following this procedure, the M2 fractional wave eigenvalues of the
 158 groundwater level for each of the four seismic events (Table 1) were calculated and
 159 the results are shown in Figure 5.



160

161 **Figure 5. M2 fractional wave eigenvalues in four seismic events at the Lugu Lake Station**

162

well water level

163 The Wenchuan earthquake (05/12/2008, Mw 7.9) shows the greatest impact on
 164 the eigenvalues of the M2 sub-wave at Lugu Lake station. Its M2 wave tidal factor
 165 decreased from 0.28 mm/uGal prior to the earthquake to 0.23 mm/uGal, especially for
 166 the relative phase, which changed from an average phase lead of 10 min prior to the
 167 earthquake to an average phase lag of 9 min after the earthquake. In addition, the M2
 168 sub-wave tidal factor size and phase lead size show an increasing trend prior to the



169 Wenchuan earthquake. It was difficult to affirm if the trend was anomalous prior to
170 the Wenchuan earthquake due to the limited pre-earthquake observation data. The
171 tidal factor size and relative phase changes were less evident in the other three
172 earthquakes.

173 4. Discussion

174 The moon, the sun, and other celestial bodies exert gravitational force on Earth's
175 mass points, which causes the volume of the Earth to change. The volume of the solid
176 skeleton of the aquifer in the Earth's crust changes accordingly, resulting in changes in
177 the aquifer's pressure head (pore pressure) and the consequent rise and fall of the
178 water level in the well. For the ideal horizontal stratified pressurized aquifer model,
179 the partial differential equation for the effect of solid tidal body strain on the pressure
180 head of the pressurized aquifer can be derived from the theory of elasticity and theory
181 of groundwater dynamics as follows:

$$\frac{\partial H}{\partial t} = \frac{K}{S_s} \nabla^2 H - \frac{1}{S_s} \frac{\partial \theta}{\partial t} \quad (2)$$

182 In the above equation, H is the pressure head within the aquifer, t is time, K
183 is the permeability coefficient of the aquifer, S_s is the unit water storage coefficient
184 of the aquifer, and θ is the solid tidal body strain. Under the condition of no drainage,
185 the simplified solution of equation (2) is:

$$H_n = \frac{-1}{S_s} \sum_i A_{ti} \cos(\omega_{ti} t - \varphi_{ti}) + H_0 \quad (3)$$

186 In the above equation, A_{ti} , ω_{ti} , φ_{ti} are the amplitude, angular frequency, and
187 initial phase of the i th harmonic of the solid tidal body strain at the moment t ,

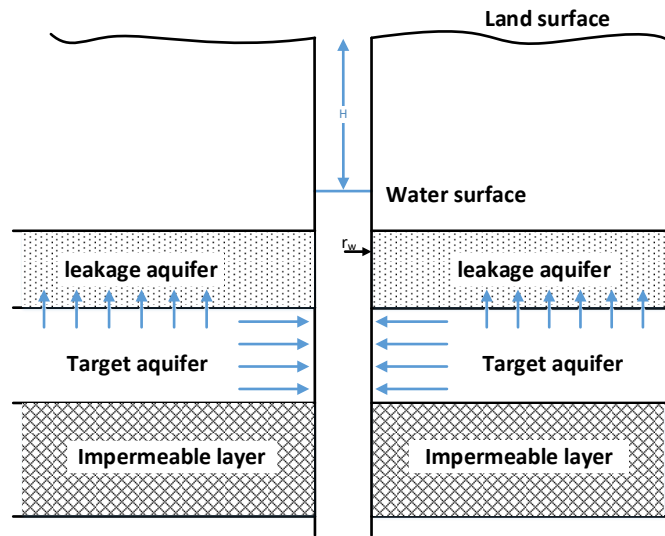


188 respectively, and H_0 is the average pressure head of the aquifer. When there is a
189 seepage influence between well-aquifer and only the case of solid tidal, an angular
190 frequency(ω) harmonic is considered, and the equation solution can be changed to:

$$H_w = H_n + H_0 \cos(\omega t + \varphi_w + \Psi) \quad (4)$$

191 Where H_w is the pressure head of the well water column in the pressurized
192 aquifer (groundwater level), φ_w is the phase angle of the groundwater level to the
193 solid tide response. It can be seen that a certain independent sub-tidal wave in the
194 groundwater level can be simplified to a sine-cosine function for calculation.

195 Regarding a well-aquifer model, the water barrier (impermeable layer) covering
196 the top of the original aquifer is changed into a leakage aquifer, i.e., a semi-confined
197 aquifer, which is a soil layer with poor permeability, and a head difference exists
198 between the aquifer and adjacent aquifer. Although the permeability of the soil layer
199 of the leaky aquifer is poor, under the condition that a head difference exists between
200 the aquifer and neighboring aquifer, water seepage between the aquifer and leaky
201 aquifer also occurs. Owing to the wide area of distribution, the total amount of water
202 is considerable. Compared with the junction area between the aquifer, interface
203 between the transgressive aquifer, and the borehole is negligible, i.e., the amount of
204 water alternation between the transgressive aquifer and borehole is negligible.



205

206

Figure 6. Well-Aquifer Modeling

207 A completely confined aquifer (Figure 6), without considering the friction and
 208 other factors, the water will directly squeeze into the borehole and its pressure will be
 209 transferred to the borehole without any loss, that raise the water level of the well. In a
 210 transgressive aquifer, the pressure within will be shared partially, affecting the
 211 efficiency of tidal response of the water level in the borehole. The efficiency of the
 212 tidal response of the groundwater level is affected by the presence of a transgressive
 213 aquifer. Compared to the simple one-dimensional well-aquifer structure, the water
 214 level in a borehole with a transgressive aquifer can be decomposed into two simple
 215 harmonic oscillations in the same direction and frequency.

$$x_1 = A_1 \cos(\omega t + \varphi_1)$$

$$x_2 = A_2 \cos(\omega t + \varphi_2)$$

(5)

216 Where x_1 is the recharge of water from the ideal aquifer to the borehole and x_2



217 is the loss of water from the aquifer to borehole owing to leakage to the
 218 semi-pressurized aquifer; the magnitude of the rise in the water level in the borehole
 219 can be expressed as $x = x_1 - x_2$:

$$\begin{aligned} x &= x_1 - x_2 \\ &= A_1 \cos(\omega t + \varphi_1) - A_2 \cos(\omega t + \varphi_2) \\ &= (A_1 \cos \varphi_1 \cos \omega t - A_1 \sin \varphi_1 \sin \omega t) - (A_2 \cos \varphi_2 \cos \omega t - A_2 \sin \varphi_2 \sin \omega t) \\ &= (A_1 \cos \varphi_1 - A_2 \cos \varphi_2) \cos \omega t - (A_1 \sin \varphi_1 - A_2 \sin \varphi_2) \sin \omega t \end{aligned}$$

220 taking $A \cos \varphi = A_1 \cos \varphi_1 - A_2 \cos \varphi_2$ and $A \sin \varphi = A_1 \sin \varphi_1 - A_2 \sin \varphi_2$

221 Then:

$$x = A \cos \varphi \cos \omega t - A \sin \varphi \sin \omega t = A \cos(\omega t + \varphi) \quad (6)$$

222 From Equation 6, it can be seen that the frequency of the synthesized simple
 223 harmonic continues in the same direction and its frequency remains unchanged. The
 224 amplitude and phase of the combined vibration are:

$$\begin{aligned} A &= \sqrt{(A \sin \varphi)^2 + (A \cos \varphi)^2} \\ &= \sqrt{(A_1 \sin \varphi_1 - A_2 \sin \varphi_2)^2 + (A_1 \cos \varphi_1 - A_2 \cos \varphi_2)^2} \quad (7) \\ &= \sqrt{A_1^2 + A_2^2 - 2A_1 A_2 \cos(\varphi_1 - \varphi_2)} \end{aligned}$$

$$\tan \varphi = \frac{A \sin \varphi}{A \cos \varphi} = \frac{A_1 \sin \varphi_1 - A_2 \sin \varphi_2}{A_1 \cos \varphi_1 - A_2 \cos \varphi_2} \quad (8)$$

225 Equation 8 shows that the phase of the combined vibration is related to the
 226 respective phases of the sub-vibrations and individual amplitude of the sub-vibration.

227 Here, we considered M_2 wave as an example, the simulations, procedure and



228 performance are shown in Table 3.

229 Table 3. Calculations for simulating the amplitude and phase of water level oscillations in wells
 230 with transgressive aquifers

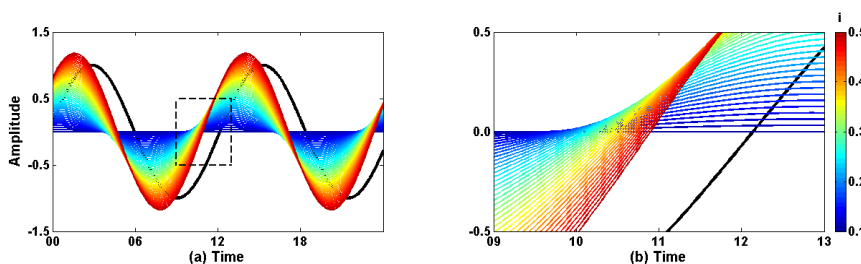
| Steps | Content | Illustrate |
|-------|--|---|
| 1 | $td = 1 \times \cos(2\pi f\tau)$ | Assuming the M2 sub-wave Earth solid tide, in which $f = 1.9324cpd$ (cpd - cycle per day) |
| 2 | $wl_{ideal} = 1 \times \cos(2\pi f\tau - 0.1\pi)$ | Groundwater level vibration under an ideal pressurized aquifer structure, which is assumed to be in phase with the solid tide with a lag of 0.1π , indicating a lag of about 37 minutes |
| 3 | $wl_{leakage_i} = 1 \times \cos(2\pi f\tau - 0.1 \times i \times \pi)$ | Assuming that the transgressive aquifer causes the groundwater level to vibrate with an amplitude of 1, except that the phase is $0.1 \times i \times \pi$ ($i = 1,2,3, \dots$) |
| 4 | $wl_{leakage_j} = 1 * j * \times \cos(2\pi f\tau - 0.2 \times \pi)$ | Assuming that the phase of the transgressive aquifer is fixed at a lag of 0.2π s, the amplitude takes the value of $1 * j$ ($j = 1, 0.9, 0.8 \dots$) |
| 5 | $wl = wl_{ideal} - wl_{leakage_i}$ | Synthetic groundwater level |

231 Considering the pressure of the target aquifer drives the recharge of the overflow
 232 aquifer, its phase will only be equal to or lag behind that of the target aquifer, and
 233 under the premise of keeping the amplitude of the overflow aquifer unchanged,
 234 $i = 1,2,3 \dots$ were considered. The corresponding values of the phases are
 235 $-0.1\pi, -0.2\pi, -0.3\pi \dots$, and the results of the calculations are as follows:



| i | Range | Phase | j | Range | Phase |
|-----|-------|--------|-----|-------|--------|
| 1 | 0 | --- | 1 | 0.313 | -1.100 |
| 2 | 0.313 | -1.100 | 0.9 | 0.313 | -0.779 |
| 3 | 0.618 | -0.942 | 0.8 | 0.344 | -0.488 |
| 4 | 0.908 | -0.785 | 0.7 | 0.398 | -0.260 |
| 5 | 1.176 | -0.628 | 0.6 | 0.468 | -0.093 |
| 6 | 1.414 | -0.471 | 0.5 | 0.547 | 0.028 |

236 Figure 7 shows $i=1$ indicates that the target aquifer pressure is all converted to
 237 the leaky aquifer; thus, the water level in the borehole will remain unchanged, which
 238 is only the ideal state. With the increase of the value of i , the phase lag in the leaky
 239 aquifer gets progressively larger, and the synthetic phase gets progressively closer to
 240 the theoretical value of the gravitational tidal phase. However, the phase is always in a
 241 "lead" state. Simultaneously, as the value of i increases, the synthesized amplitude
 242 increases in magnitude, and the magnitude may also exceeds the magnitude of the
 243 ideal pressurized aquifer structure.



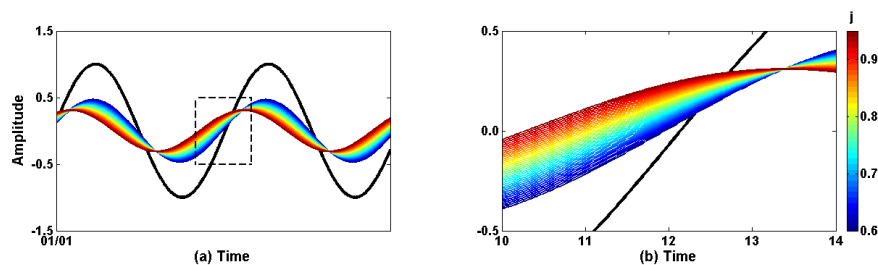
244

245 **Figure 7. Water level changes in synthetic wells when the leaky aquifer amplitude is**
 246 **held constant and phase lag shows different values**

247 Next, the phase value of the leaky aquifer is fixed (here, it is fixed to -0.2π ,



248 lagging behind the theoretical value of gravity tides by 0.2π). Its amplitude is
249 changed by $j = 1, 0.9, 0.8 \dots$, from the calculation results (Figure 8), the synthetic
250 vibration phase lead becomes progressively smaller as the value of j decreases.
251 Nevertheless, the synthetic vibration phases lead the theoretical solid-tide phases
252 under the prerequisite of $j > 0.5$, and lagging occurs only when the phase of synthetic
253 vibration is $j < 0.5$; the synthetic vibration phase lags. Simultaneously, as the value of
254 j decreases, the amplitude of the synthetic vibration progressively increases.



255

256 **Figure 8. Water level changes in synthetic borehole when the phase lag of the leaky**
257 **aquifer is held constant and the magnitude varies**

258 The results shown in Figure 7&8 clearly show that closer the phase and
259 amplitude of the leaky aquifer are to those of the ideal aquifer, the more the phase of
260 its synthetic vibration lead to the theoretical solid gravity tide.

261 5. Conclusions

262 Based on the theoretical calculation our results show the large phase lag of the
263 leaky aquifer, the closer the synthetic phase to the theoretical value of gravity tidal
264 phase. But the phase always remains "phase lead"; simultaneously, the synthetic
265 amplitude increased progressively, and the amplitude may even exceed that of the
266 ideal pressurized aquifer structure. In addition, the smaller the oscillation amplitude of



267 the leaky aquifer, the smaller the synthetic vibration phase lead. However, under the
268 premise of $j > 0.5$ (j is the amplitude ratio of the leaky aquifer relative to the ideal
269 aquifer), the synthetic vibration phase lead was in excess to the theoretical solid tidal
270 phase. The synthetic vibration phase lag occurred only when $j \leq 0.5$. Meanwhile, the
271 synthetic vibration amplitude became progressively larger as the value of j decreased.

272 The Wenchuan earthquake caused the M2-wave tidal factor of the water level in
273 the Lugu Lake Station well to decrease from 0.28 mm/uGal prior to the earthquake to
274 0.23 mm/uGal; the phase lead from an average of 10 min of pre-seismic overshooting
275 to an average of 9 min of post-seismic lagging. The pre-earthquake phase leads over
276 the theoretical gravity tide, indicates the existence of a leaky aquifer in the Lugu Lake
277 well. After the earthquake, the phase changed from lead to lag, which can only be due
278 to either the disappearance of the leaky aquifer or lagging of the synthetic vibrational
279 phase because the amplitude ratio of the leaky aquifer relative to the ideal aquifer is
280 ≤ 0.5 . The leaky aquifer, as an actual aquifer, cannot disappear because of the
281 earthquake. However, the earthquake can only change the amplitude ratio of the leaky
282 aquifer relative to the ideal aquifer.

283 The Wenchuan earthquake caused an increase in the permeability of the aquifer
284 in the water wells of Lugu Lake station, and this increase may be due to the
285 development of new fractures in the aquifer (Tokunaga, 1999; Zhang et al., 2019; Sun
286 et al., 2015) that enhances the permeability owing to the scouring of the fracture water
287 in the aquifer caused by the seismic wave (Yoshimi and Oh-Oka, 1975; Dobry et al.,
288 1982; Vucetic, 1994; Hsu and Vucetic, 2004; Lai et al., 2004; Wang and Manga, 2010).
289 Owing to the new fractures, the former shows a permanent increase in permeability.
290 Simultaneously, the latter will accumulate over time and revert back to the original



291 level in the aquifer because of the accumulation of groundwater minerals. From the
292 effect of several earthquakes, except for the Wenchuan earthquake, which caused the
293 groundwater level to step up, the subsequent earthquakes caused the groundwater
294 level to step down. However, the Wenchuan earthquake changed the permeability of
295 the Lugu Lake well aquifer, which did not return to the pre-earthquake level, in line
296 with the permanent increase in permeability and development of new fissures.
297 Furthermore, the other three earthquakes did not show a permanent change in
298 permeability and development of new fissures.

299 The Wenchuan earthquake led to the generation of new fissures in the Lugu Lake,
300 which led to the conduction of deep high-pressure water into the aquifer, resulting in a
301 co-seismic response of step-up; the subsequent earthquakes did not generate new
302 fissures but seismic waves only caused fissure water flushing that enhanced the
303 permeability of the aquifer and a step-down in the water level of the borehole when
304 boreholes were close to the discharge zone (He and Singh, 2018). The M2 fractional
305 wave tidal factor size and phase lead size prior to the Wenchuan earthquake showing
306 an increasing trend; however, the anomalous nature of this trend prior to the
307 Wenchuan earthquake can not be affirmed due to the limited pre-earthquake
308 observation data.

309 **Declaration of Competing Interest**

310 The authors declare that they have no known competing financial interests or
311 personal relationships that could have appeared to influence the work reported in this
312 paper.

313 **Code/Data availability**



314 At present, data and code can only be submitted to reviewers in the form of
315 attachments.

316 **Author contribution**

317 Anhua He carry out the design of the manuscript ideas, Yang Liu & Fan Zhang
318 completed data collection and editing work, Haixia Sun completed partial code,
319 Yanzhang Wang and Ramesh P. Singh review and improve the manuscript.

320 **Acknowledgments**

321 The present study was supported financially by National Natural Science
322 Foundation of China (41772256) and National Key R&D Program of China,
323 (2018YFC1503803). The authors thank the China Earthquake Network Center for
324 providing the water-level data and the United States Geological Survey for providing
325 the seismic data.

326 **【References】**

327 Allègre, V., Brodsky, E. E., Xue, L., Nale, S. M., Parker, B. L., & Cherry, J. A. (2016).

328 Using earth - tide induced water pressure changes to measure in situ
329 permeability: A comparison with long - term pumping tests. *Water Resources*
330 *Research*, 52(4), 3113-3126.

331 Arditty, P. C., Ramey Jr, H. J., & Nur, A. M. (1978, October). Response of a closed
332 well-reservoir system to stress induced by earth tides. In *SPE Annual Technical*
333 *Conference and Exhibition?* (pp. SPE-7484). SPE.

334 Bredehoeft, J. D. (1967). Response of well - aquifer systems to Earth tides. *Journal of*



- 335 Geophysical Research, 72(12), 3075-3087.
- 336 Burbey, T. J. (2010). Fracture characterization using Earth tide analysis. Journal of
337 Hydrology, 380(3-4), 237-246.
- 338 Cooper Jr, H. H., Bredehoeft, J. D., Papadopoulos, I. S., & Bennett, R. R. (1965). The
339 response of well - aquifer systems to seismic waves. Journal of Geophysical
340 Research, 70(16), 3915-3926.
- 341 Ding, F. H., Han, X. L., Ha, Y. Y., & Dai Yong, L. Y. (2015). Relationship of porosity
342 and volume compression coefficient of solid skeleton and water in artesian well
343 aquifer. Earth Science: Journal of China University of Geosciences, 40(7),
344 1248-1253.
- 345 Dobry, R., Ladd, R. S., Yokel, F. Y., Chung, R. M., & Powell, D. (1982). Prediction of
346 pore water pressure buildup and liquefaction of sands during earthquakes by the
347 cyclic strain method (Vol. 138, p. 150). Gaithersburg, MD: National Bureau of
348 Standards.
- 349 Elkhoury, J. E., Brodsky, E. E., & Agnew, D. C. (2006). Seismic waves increase
350 permeability. Nature, 441(7097), 1135-1138.
- 351 Gao, X., Sato, K., & Horne, R. N. (2020). General solution for tidal behavior in
352 confined and semiconfined aquifers considering skin and wellbore storage effects.
353 Water Resources Research, 56(6), e2020WR027195.
- 354 Gulley, A. K., Ward, N. F. D., Cox, S. C., & Kaipio, J. P. (2013). Groundwater
355 responses to the recent Canterbury earthquakes: a comparison. Journal of



- 356 Hydrology, 504, 171-181.
- 357 He, A., Deng, W., Singh, R. P., & Lyu, F. (2020). Characteristics of hydroseismograms
358 in Jingle well, China. *Journal of Hydrology*, 582, 124529.
- 359 He, A., Fan, X., Zhao, G., Liu, Y., Singh, R. P., & Hu, Y. (2017). Co-seismic response
360 of water level in the Jingle well (China) associated with the Gorkha Nepal (Mw
361 7.8) earthquake. *Tectonophysics*, 714, 82-89.
- 362 He, A., & Singh, R. P. (2019). Groundwater level response to the Wenchuan
363 earthquake of May 2008. *Geomatics, Natural Hazards and Risk*, 10(1), 336-352.
- 364 He, A., Singh, R. P., Sun, Z., Ye, Q., & Zhao, G. (2016). Comparison of regression
365 methods to compute atmospheric pressure and earth tidal coefficients in water
366 level associated with Wenchuan Earthquake of 12 May 2008. *Pure and Applied
367 Geophysics*, 173, 2277-2294.
- 368 Hsieh, P. A., Bredehoeft, J. D., & Farr, J. M. (1987). Determination of aquifer
369 transmissivity from Earth tide analysis. *Water resources research*, 23(10),
370 1824-1832.
- 371 Hsu, C. C., & Vucetic, M. (2004). Volumetric threshold shear strain for cyclic
372 settlement. *Journal of geotechnical and geoenvironmental engineering*, 130(1),
373 58-70.
- 374 Lai, G., Ge, H., Xue, L., Brodsky, E. E., Huang, F., & Wang, W. (2014). Tidal
375 response variation and recovery following the Wenchuan earthquake from water
376 level data of multiple wells in the nearfield. *Tectonophysics*, 619, 115-122.



- 377 Lee, S. H., Cheong, J. Y., Park, Y. S., Ha, K., Kim, Y., Kim, S. W., & Hamm, S. Y.
378 (2017). Groundwater level changes on Jeju Island associated with the Kumamoto
379 and Gyeongju earthquakes. *Geomatics, Natural Hazards and Risk*, 8(2),
380 1783-1791.
- 381 Liu CP, Liao X, Shi Y, Tang YD. 2017. Crustal stress and groundwater dynamic
382 response (in Chinese). Beijing: Seismological Press.
- 383 Ma, Y., Wang, G., Shi, Z., Yan, R., & Yu, H. (2023). Groundwater level and
384 temperature changes following the great Tangshan earthquake of 1976 near the
385 epicenter. *Geomatics, Natural Hazards and Risk*, 14(1), 2197103.
- 386 Maas, C., & De Lange, W. J. (1987). On the negative phase shift of groundwater tides
387 near shallow tidal rivers—The Gouderak anomaly. *Journal of Hydrology*, 92(3-4),
388 333-349.
- 389 Pawlowicz, R., Beardsley, B., & Lentz, S. (2002). Classical tidal harmonic analysis
390 including error estimates in MATLAB using T_TIDE. *Computers & Geosciences*,
391 28(8), 929-937.
- 392 Rasmussen, T. C., & Crawford, L. A. (1997). Identifying and removing barometric
393 pressure effects in confined and unconfined aquifers. *Groundwater*, 35(3),
394 502-511.
- 395 Sato, M., Fujita, S., Saito, A., Ikeda, Y., Kitazawa, H., Takahashi, M., ... & Aizawa, Y.
396 (2006). Increased incidence of transient left ventricular apical ballooning
397 (so-called Takotsubo cardiomyopathy) after the mid-Niigata Prefecture
398 earthquake. *Circulation journal*, 70(8), 947-953.



- 399 Shi, Z., Wang, G., Wang, C. Y., Manga, M., & Liu, C. (2014). Comparison of
400 hydrological responses to the Wenchuan and Lushan earthquakes. *Earth and*
401 *Planetary Science Letters*, 391, 193-200.
- 402 Sun, X., Wang, G., & Yang, X. (2015). Coseismic response of water level in
403 Changping well, China, to the Mw 9.0 Tohoku earthquake. *Journal of Hydrology*,
404 531, 1028-1039.
- 405 Tokunaga, T. (1999). Modeling of earthquake-induced hydrological changes and
406 possible permeability enhancement due to the 17 January 1995 Kobe Earthquake,
407 Japan. *Journal of Hydrology*, 223(3-4), 221-229.
- 408 Toll, N. J., & Rasmussen, T. C. (2007). Removal of barometric pressure effects and
409 earth tides from observed water levels. *Groundwater*, 45(1), 101-105.
- 410 Van der Kamp, G., & Gale, J. E. (1983). Theory of earth tide and barometric effects in
411 porous formations with compressible grains. *Water Resources Research*, 19(2),
412 538-544.
- 413 Vucetic, M. (1994). Cyclic threshold shear strains in soils. *Journal of Geotechnical*
414 *engineering*, 120(12), 2208-2228.
- 415 Wang, C. Y., Doan, M. L., Xue, L., & Barbour, A. J. (2018). Tidal response of
416 groundwater in a leaky aquifer—Application to Oklahoma. *Water Resources*
417 *Research*, 54(10), 8019-8033.
- 418 Wang C. Y., Manga M. 2010. Earthquakes and water. *Lecture Notes in Earth Sciences*
419 114, Berlin: Springer-Verlag.



- 420 Wood, M. D., Allen, R. V., & Allen, S. S. (1973). Methods for prediction and
421 evaluation of tidal tilt data from borehole and observatory sites near active faults.
422 Philosophical Transactions for the Royal Society of London. Series A,
423 Mathematical and Physical Sciences, 245-252.
- 424 Xue, L., Li, H. B., Brodsky, E. E., Xu, Z. Q., Kano, Y., Wang, H., ... & Huang, Y.
425 (2013). Continuous permeability measurements record healing inside the
426 Wenchuan earthquake fault zone. *Science*, 340(6140), 1555-1559.
- 427 Yan, R., Wang, G., Ma, Y., Shi, Z., & Song, J. (2020). Local groundwater and tidal
428 changes induced by large earthquakes in the Taiyuan Basin, North China from
429 well monitoring. *Journal of Hydrology*, 582, 124479.
- 430 Yan, X., Shi, Z., Wang, G., Zhang, H., & Bi, E. (2021). Detection of possible
431 hydrological precursor anomalies using long short-term memory: A case study of
432 the 1996 Lijiang earthquake. *Journal of Hydrology*, 599, 126369.
- 433 Yoshimi, Y., & Oh-oka, H. (1975). Influence of degree of shear stress reversal on the
434 liquefaction potential of saturated sand. *Soils and foundations*, 15(3), 27-40.
- 435 Zhang, S., Shi, Z., & Wang, G. (2019). Comparison of aquifer parameters inferred
436 from water level changes induced by slug test, earth tide and earthquake—A case
437 study in the three Gorges area. *Journal of Hydrology*, 579, 124169.
- 438 Zhang, Z. D., Wang, C. W., & Gao, Y. B. (1991). The relationship between variation
439 of radius in the well Shandong Province No. 7 and response to Earth tide.
440 *Chinese Journal of Geophysics*, 34(2), 203-209.
- 441 Zhou, K. G., Li, S. L., Tan, S. L., Li, H., Rong, J. D., et al. (1993). On phase shift in



442 observation of tidal fluctuation in a deep well. *Crustal Deformation and*
443 *Earthquake*, 13(3), 18-24.

444 Zhu, A. Y. (2021). Unsaturated Flow Influences the Response of Leaky Aquifer to
445 Earth Tides. *Lithosphere*, 2021(Special 3), 6415482.

446 Zhu, J. B., Kang, J. Q., Elsworth, D., Xie, H. P., Ju, Y., & Zhao, J. (2021). Controlling
447 induced earthquake magnitude by cycled fluid injection. *Geophysical Research*
448 *Letters*, 48(19), e2021GL092885.